

The Impact of Secondary non-Gaussianities in the CMB on Cosmological Parameter Estimation

Joseph Smidt, Shahab Joudaki, Alexandre Amblard, Paolo Serra, and Asantha Cooray
Center for Cosmology, Department of Physics and Astronomy, University of California, Irvine, CA 92697

We consider corrections to the underlying cosmology due to secondary contributions from weak gravitational lensing, the integrated Sachs-Wolfe effect, and the Sunyaev-Zel'dovich effect contained in the trispectrum. We incorporate these additional contributions to the covariance of a binned angular power spectrum of temperature anisotropies in the analysis of current and prospective data sets. Although recent experiments such as ACBAR and CBI are not particularly sensitive to these additional non-Gaussian effects, the interpretation of Planck and CMBPol anisotropy spectra will require an accounting of non-Gaussian covariance leading to a degradation in cosmological parameter estimates by up to 20% and 30%, respectively.

PACS numbers: 98.80.-k 98.70.Vc 98.80.Es

I. INTRODUCTION

The cosmic microwave background's (CMB) ability to constrain the cosmological parameters has driven a large variety of CMB experiments. The high quality measurements of the temperature and polarization of the CMB are compatible with a flat universe with nearly scale invariant fluctuations. The sensitivity to small angular scales of recent experiments such as WMAP5 [1], ACBAR [2] and CBI [3] give us a better understanding of anisotropies from local large scale structure (LSS) and from non-linear effects such as weak gravitational lensing. The non-Gaussianity of these fluctuations can have an effect in the estimation of the cosmological parameters, especially for future experiments. However, possible non-Gaussian effects have not been considered in previous analyses, under the assumption that they are negligible.

Non-Gaussianities show up as contributions to the four-point correlation function, or trispectrum in Fourier space, of the CMB temperature fluctuations [4, 5]. The four point correlations quantify the sample variance and covariance of the two point correlation of power spectrum measurements [6, 7]. To adequately understand the statistical measurements of CMB anisotropy fluctuations a proper understanding of the four point contributions is needed. Given the high precision level of cosmological parameter measurements by current and future surveys, a careful consideration must be attached to understanding the presence of non-Gaussian signals at the four point level. The goal of this paper is to understand to what extent these non-Gaussianities affect constraints on the cosmological parameters

As explored in previous work (e.g. [8–11]), one of the most important non-linear contributions to CMB temperature fluctuations results from weak gravitational lensing. Contributions to the four point level arise from the non-linear mode-coupling nature of the lensing effect, as well as correlations between weak lensing angular deflections and secondary effects that trace the same large scale structure. The trispectrum due to lensing alone is

studied in [5], and further considered under an all-sky formulation in [4].

In our analysis we include contributions to the trispectrum from three well known secondary sources. First, we consider the contribution of the trispectrum to the power spectrum covariance due to lensing. We also consider contributions from the integrated Sachs-Wolfe effect (ISW; [12]) and the Sunyaev-Zel'dovich effect (SZ; [13]), both which cross-correlate with lensing to produce non-Gaussianity. Each of these effects becomes non-negligible on small angular scales and must be taken into account for a more complete treatment of cosmological parameter constraints.

In a situation without instrumental noise, the lensing contribution to the trispectrum can increase the values along the diagonal of the covariance matrix on the order of about 10% [14]. The SZ contributions are greater than the lensing by as much as an order of magnitude. However, with noise added follows the possibility that these effects on the trispectrum become negligible. Most experiments thus far have been too noisy at small angular scales to observe these non-Gaussian effects on the cosmological parameters. We explore how firmly this holds for the ACBAR and CBI data sets when combined with WMAP five-year data as well for future Planck and CMBPol measurements.

Moreover, we consider the weak lensing scaling parameter A_L in our analysis. This parameter scales the power spectrum of the CMB lensing potential $C_l^{\phi\phi}$ such that $A_L = 0$ corresponds to an unlensed scenario, whereas $A_L = 1$ renders the expected lensed result. It was first reported that in an analysis of the ACBAR data set this parameter is incompatible with the expected value of $A_L = 1$ at 2.5σ [15]. ACBAR has since updated their data set with a new calibration, and the ACBAR team finds that the amplitude is consistent with the expected value of unity [16]. However, given that this parameter is sensitive to physics at high multipoles, such as that encapsulated in the trispectrum, we also include A_L as an extra parameter in our calculations.

Our analysis of the ACBAR and CBI data sets, com-

binned with WMAP 5-year data, show that secondary contributions in the trispectrum have a negligible effect on the uncertainties of the cosmological parameters. At most the constraints on the cosmological parameters change by no more than 10%. We find that these modifications are negligible due to the increase in noise at large multipoles (as shown in Fig. 5).

However, in a mock Planck data set with realistic noise contributions, the non-Gaussian effects coming from the trispectrum become more important, with error constraint degradations up to 20% (as shown in Table IV). For the case of CMBPol this rises to $\lesssim 30\%$. For this reason, future experiments with at least Planck-level sensitivity at high l should consider non-Gaussianities from the trispectrum in order to have proper error bar estimates.

Lastly, we show A_L to be consistent with the expected value of unity, primarily due to the same reasons that Ref. [16] found it to be consistent with the theoretically expected value. If we had used the original ACBAR dataset, prior to their most recent update, we find that A_L is inconsistent with unity at the same confidence as found by Ref. [15]. We also find that this parameter remains consistent with unity when both trispectrum effects and the running $dn_s/dlnk$ of the spectral index n_s are included in the analysis.

In §II, we review the calculation for the trispectrum contribution to the covariance matrix. In §III, we calculate the impact of the trispectrum on the cosmological parameters for current and future experiments considering a set of parameter configurations. The fiducial cosmologies considered can be found in Table I. In §IV, we conclude with a summary.

II. ANALYSIS

A. Lensing Trispectrum

We begin with a review of how to calculate the various contributions of the trispectrum to the covariance matrix. For a comprehensive introduction and derivation of these equations, see [14].

In the flat sky approximation, the power spectrum and trispectrum are defined via:

$$\begin{aligned} \langle \Theta^t(\mathbf{l}_1)\Theta^t(\mathbf{l}_2) \rangle &= (2\pi)^2 \delta_D(\mathbf{l}_{12}) C_l^\Theta, \\ \langle \Theta^t(\mathbf{l}_1) \dots \Theta^t(\mathbf{l}_4) \rangle_c &= (2\pi)^2 \delta_D(\mathbf{l}_{1234}) T^\Theta(\mathbf{l}_1, \mathbf{l}_2, \mathbf{l}_3, \mathbf{l}_4). \end{aligned} \quad (1)$$

In computing these quantities the band powers are obtained, as

$$C_i = \int_{s_i} \frac{d^2 l W_i}{A_{s_i}} \frac{l^2}{2\pi} \Theta(\mathbf{l}) \Theta(-\mathbf{l}), \quad (2)$$

where $A_{s_i} \equiv A_s(l_i) = \int d^2 l W_i$ is the area of 2D shell in multipole space, W_i is the i^{th} window function and the

subscript s_i stands for the i^{th} shell in multipole space over which we are integrating. The signal covariance matrix C_{ij} is given by

$$\begin{aligned} C_{ij} &= \frac{1}{A} \left[\frac{(2\pi)^2}{A_{s_i}} 2C_i^2 + T_{ij}^\Theta \right], \\ T_{ij}^\Theta &= \int \frac{d^2 l_i W_i}{A_{s_i}} \int \frac{d^2 l_j W_j}{A_{s_j}} \frac{l_i^2 l_j^2}{(2\pi)^2} T^\Theta(\mathbf{l}_i, -\mathbf{l}_i, \mathbf{l}_j, -\mathbf{l}_j) \end{aligned} \quad (3)$$

where A is the survey area in steradians. The first term of the covariance matrix C_{ij} is the Gaussian contribution to the sample variance and includes, in addition to the primary component, contributions through lensing and secondary effects. The second term T_{ij} represents the non-Gaussian contributions contained in the trispectrum.

The surveys we consider also include instrumental noise. The noise is incorporated into our Gaussian variance as an additional contribution to the power spectrum

$$C_l^t = C_l^\Theta + N_l \quad (5)$$

where N_l is the power spectrum of the detector and other sources of noise introduced by the experiment. These noise contributions are included in respective experiment's publicly released data and significantly impact the covariance matrix, in particular on small angular scales.

For the power spectrum covariance, we are interested in the case where $\mathbf{l}_2 = -\mathbf{l}_1$ with $|\mathbf{l}_1| = l_i$, and $\mathbf{l}_4 = -\mathbf{l}_3$ with $|\mathbf{l}_3| = l_j$. These conditions render parallelograms for the trispectrum configuration in Fourier space.

To account for the lensing contribution to the trispectrum, we must compute

$$\begin{aligned} T^\Theta(\mathbf{l}_i, -\mathbf{l}_i, \mathbf{l}_j, -\mathbf{l}_j) &= \\ C_{l_i}^\Theta C_{l_i}^\Theta &\left[C_{|\hat{\mathbf{l}}_i + \hat{\mathbf{l}}_j|}^{\phi\phi} \left[(\hat{\mathbf{l}}_i + \hat{\mathbf{l}}_j) \cdot \hat{\mathbf{l}}_i \right]^2 + C_{|\hat{\mathbf{l}}_i - \hat{\mathbf{l}}_j|}^{\phi\phi} \left[(\hat{\mathbf{l}}_i - \hat{\mathbf{l}}_j) \cdot \hat{\mathbf{l}}_i \right]^2 \right] \\ + C_{l_j}^\Theta C_{l_j}^\Theta &\left[C_{|\hat{\mathbf{l}}_i + \hat{\mathbf{l}}_j|}^{\phi\phi} \left[(\hat{\mathbf{l}}_i + \hat{\mathbf{l}}_j) \cdot \hat{\mathbf{l}}_j \right]^2 + C_{|\hat{\mathbf{l}}_i - \hat{\mathbf{l}}_j|}^{\phi\phi} \left[(\hat{\mathbf{l}}_i - \hat{\mathbf{l}}_j) \cdot \hat{\mathbf{l}}_j \right]^2 \right] \\ + 2C_{l_i}^\Theta C_{l_j}^\Theta &\left[C_{|\hat{\mathbf{l}}_i + \hat{\mathbf{l}}_j|}^{\phi\phi} (\hat{\mathbf{l}}_i + \hat{\mathbf{l}}_j) \cdot \hat{\mathbf{l}}_i (\hat{\mathbf{l}}_i + \hat{\mathbf{l}}_j) \cdot \hat{\mathbf{l}}_j \right. \\ &\left. - C_{|\hat{\mathbf{l}}_i - \hat{\mathbf{l}}_j|}^{\phi\phi} (\hat{\mathbf{l}}_i - \hat{\mathbf{l}}_j) \cdot \hat{\mathbf{l}}_i (\hat{\mathbf{l}}_i - \hat{\mathbf{l}}_j) \cdot \hat{\mathbf{l}}_j \right], \end{aligned} \quad (6)$$

where $C_{l_i}^\Theta$ is the TT power spectrum and $C_{l_i}^{\phi\phi}$ is the lensing power spectrum. This equation includes all terms with no additional permutations. Similarly, for the lensing-secondary trispectrum effects, such as lensing-

ISW and lensing-SZ, we calculate

$$\begin{aligned}
T^\Theta(\mathbf{l}_i, -\mathbf{l}_i, \mathbf{l}_j, -\mathbf{l}_j) = & \\
& 2(\mathbf{l}_i \cdot \mathbf{l}_j)^2 \left[\left(C_{l_i}^{\phi s} \right)^2 C_{l_j}^\Theta + \left(C_{l_j}^{\phi s} \right)^2 C_{l_i}^\Theta \right] \\
& - \left[\mathbf{l}_i \cdot (\mathbf{l}_i + \mathbf{l}_j) \right]^2 \left(C_{l_i}^{\phi s} \right)^2 + \left[\mathbf{l}_j \cdot (\mathbf{l}_i + \mathbf{l}_j) \right]^2 \left(C_{l_j}^{\phi s} \right)^2 \right] C_{|\mathbf{l}_i + \mathbf{l}_j|}^\Theta \\
& - \left[\mathbf{l}_i \cdot (\mathbf{l}_i - \mathbf{l}_j) \right]^2 \left(C_{l_i}^{\phi s} \right)^2 + \left[\mathbf{l}_j \cdot (\mathbf{l}_i - \mathbf{l}_j) \right]^2 \left(C_{l_j}^{\phi s} \right)^2 \right] C_{|\mathbf{l}_i - \mathbf{l}_j|}^\Theta \\
& + 2[\mathbf{l}_i \cdot (\mathbf{l}_j - \mathbf{l}_i)][\mathbf{l}_j \cdot (\mathbf{l}_j - \mathbf{l}_i)] C_{l_i}^{\phi s} C_{l_j}^{\phi s} C_{|\mathbf{l}_j - \mathbf{l}_i|}^\Theta \\
& - 2[\mathbf{l}_i \cdot (\mathbf{l}_i + \mathbf{l}_j)][\mathbf{l}_j \cdot (\mathbf{l}_i + \mathbf{l}_j)] C_{l_i}^{\phi s} C_{l_j}^{\phi s} C_{|\mathbf{l}_i + \mathbf{l}_j|}^\Theta
\end{aligned}$$

where the s is a place holder denoting either the ISW or SZ contribution.

B. SZ Trispectrum

In addition to the lensing contributions to the trispectrum above, we consider contributions from the inverse Compton scattering of the CMB photons. The SZ contribution to the trispectrum is given by [17, 25]:

$$\begin{aligned}
T_{ij}^\Theta = & g_\nu^4 \int_0^{z_{\max}} dz \frac{dV}{dz} \int_{M_{\min}}^{M_{\max}} dM \frac{dn(M, z)}{dM} \\
& \times |\tilde{y}_i(M, z)|^2 |\tilde{y}_j(M, z)|^2,
\end{aligned} \quad (8)$$

where g_ν is the spectral function of the SZ effect, $V(z)$ is the comoving volume of the universe integrated to a redshift of $z_{\max} = 4$, M is the virial mass such that $[\log_{10}(M_{\min}), \log_{10}(M_{\max})] = [11, 16]$, dn/dM is the

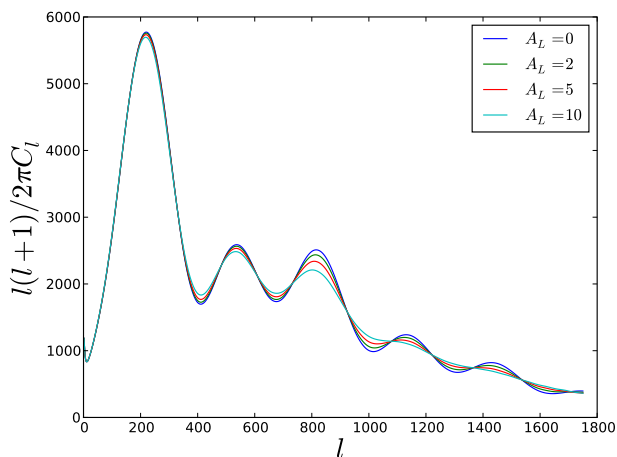


FIG. 1: The impact of varying the lensing scaling parameter on the lensed CMB temperature power spectrum, for $A_L = [0, 2, 5, 10]$.

mass function of dark matter halos as rendered by [18] utilizing the linear transfer function of [19], and \tilde{y} is the dimensionless two-dimensional Fourier transform of the projected Compton y -parameter, given via the Limber approximation [20] by:

$$\tilde{y}_l = \frac{4\pi r_s}{l_s^2} \int_0^\infty dx x^2 y_{3D}(x) \frac{\sin(lx/l_s)}{lx/l_s}, \quad (9)$$

(7) where the scaled radius $x = r/r_s$ and $l_s = d_A/r_s$ such that d_A is the angular diameter distance and r_s is the scale radius of the three-dimensional radial profile y_{3D} of the Compton y -parameter. This profile is a function of the gas density and temperature profiles as modeled in [21]. Hence, we incorporate the contributions obtained from the SZ effect along with those from lensing, lensing-ISW, and lensing-SZ effects to the covariance matrix in Eqn. 3.

C. The Weak Lensing Scaling Parameter A_L

To first order in ϕ , the weak lensing of the CMB anisotropy trispectrum can be expressed as the convolution of the power spectrum of the unlensed temperature C_l and that of the weak lensing potential $Cl^{\phi\phi}$ [15, 22, 23]. The magnitude of the lensing potential power spectrum can be parameterized by the scaling parameter A_L , defined as

$$C_l^{\phi\phi} \rightarrow A_L C_l^{\phi\phi}. \quad (10)$$

Thus, A_L is a measure of the degree to which the expected amount of lensing appears in the CMB, such that a theory with $A_L = 0$ is devoid of lensing, while $A_L = 1$ renders a theory with the canonical amount of lensing. Any inconsistency with unity represents an unexpected amount of lensing that needs to be explained with new physics, such as dark energy or modified gravity [15, 24]. The impact of this scaling parameter on the lensed CMB temperature power spectrum can be seen in Fig. 1. Qualitatively, A_L smoothes out the peaks in the power spectrum and can therefore also be viewed as a smoothing parameter in addition to its scaling property. Given that A_L primarily affects the temperature power spectrum on small angular scales, we also explore the possibility that it deviates from unity as secondary non-Gaussianities are accounted for in the analysis.

	ACBAR	CBI
H_0	72.0	73.2
$\Omega_b h^2$	0.02282	0.02291
$\Omega_c h^2$	0.1108	0.1069
τ	0.088	0.086
n_s	0.964	0.960
Δ_R^2	2.41×10^{-9}	2.09×10^{-9}

TABLE I: Fiducial model used to generate $C_{l_i}^\Theta$ and $C_{l_i}^{\phi\phi}$ in CAMB for ACBAR and CBI.

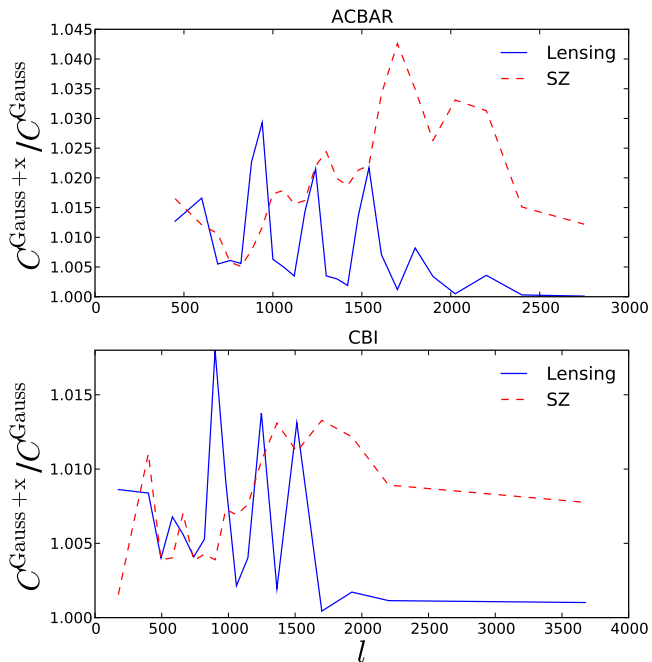


FIG. 2: The ratio of the diagonal of the covariance matrix plus trispectrum effects with the diagonal of the covariance matrix neglecting trispectrum contributions for ACBAR (top) and CBI (bottom). The x in the $C_l^{\text{Gauss}+x}$ is the specific contribution being added. We see that both the combined lensing effects and SZ alter the covariance matrix by at most a few percent. The choppiness is due to two issues: the covariance matrices provided by ACBAR and CBI are not smooth and the window functions used to bin the data take on different shapes and are themselves not smooth.

III. RESULTS

A. Analysis Using ACBAR and CBI Data

We compute $C_{l_i}^\Theta$ and $C_{l_i}^{\phi\phi}$, separately for each aforementioned experiment by utilizing the publicly available¹

Fortran code CAMB [27] for the fiducial models found in Table I. These fiducial models were taken from NASA’s Lambda website² which houses many best fit fiducial models derived from several different data sets. From these spectra, we use Eqns. 6–8 to determine the trispectrum contributions from lensing, lensing-ISW, lensing-SZ, and SZ effects. We then add each corresponding trispectrum contribution to each experiment’s publicly available covariance matrix.

For our analysis, we use the same multipole binning as the aforementioned experiments, which are obtained from the window functions plotted in Fig. 4. These window functions force proper normalized bins when we integrate over l space. To factor in the area of each survey, we note that the ACBAR survey covers 600 sq. degrees and CBI covers 143 sq. degrees.

Fig. 2 shows the diagonal ratio of the covariance matrix together with non-Gaussian contributions, with the purely Gaussian covariance matrix, for the ACBAR and CBI surveys. We plot only the diagonal, as these entries are several orders of magnitude larger than the off-diagonal pieces. All contributions along the diagonal of the covariance leave corrections no larger than on the order of 1%.

Cross-correlations become significant when the trispectrum is considered, since a fully Gaussian theory should not have any cross-correlation terms in the covariance of the temperature power spectrum. As seen in Fig. 3, the non-Gaussian corrections to the cross-correlations lie on the order of a factor of 100 as they correct off-diagonal terms that otherwise are negligible. However, as will be shown, despite the large corrections to the cross-correlations, the trispectrum effects on the cosmological parameters are negligible.

Having obtained corrections to the binned covariance matrix from trispectrum effects, we now compute the impact of these on the cosmological parameter constraints. The method we use in our analysis is based on the publicly available Markov Chain Monte Carlo (MCMC) package CosmoMC [29] with a convergence diagnostic done through the Gelman and Rubin statistics. We sample the following seven-dimensional set of cosmological parameters, adopting flat priors on them: the baryon and cold dark matter densities Ω_b and Ω_c , the ratio of the sound horizon to the angular diameter distance at the decoupling, θ_s , the scalar spectral index n_s , the overall normalization of the spectrum A_s at $k = 0.002 \text{ Mpc}^{-1}$, the optical depth to reionization, τ , and the weak lensing parameter A_L . We use the same window functions and band powers supplied from the considered experiments (see Fig. 4). We only use the band powers for $l > 900$ for both ACBAR and CBI in our CosmoMC analysis, and use WMAP data for calculations on larger angular scales. The non-Gaussian contributions to the trispec-

¹ <http://camb.info/>

² <http://lambda.gsfc.nasa.gov/>

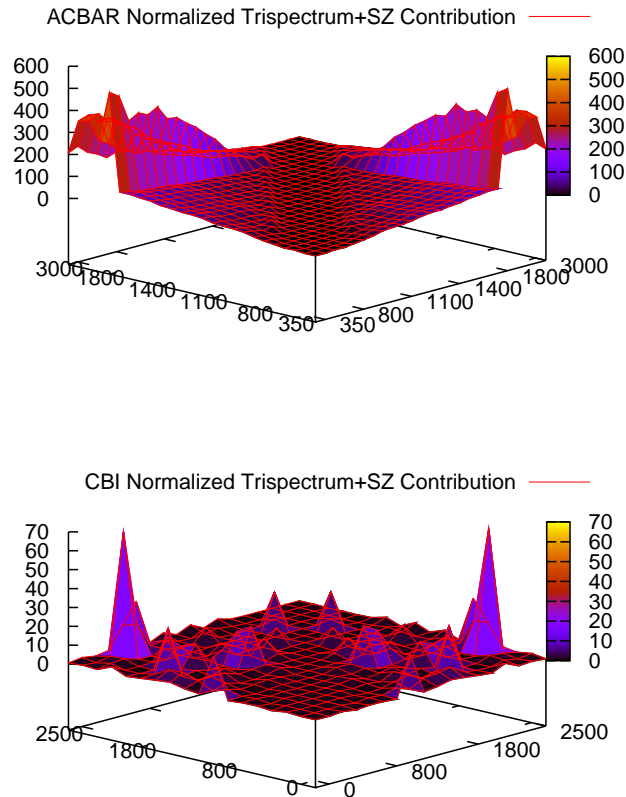


FIG. 3: The absolute values of the Gaussian covariance plus trispectrum matrix divided by the Gaussian covariance matrix alone. In the top figure we show corrections to the ACBAR data set, and in the lower figure to the CBI data set. The trispectrum contribution to the cross-correlations is about 100 times larger than the Gaussian contribution.

trum are incorporated into the binned covariance matrix for use in CosmoMC.

Table II shows the extent to which the trispectrum contributions affect the constraints on cosmological parameters for ACBAR and CBI data sets combined with WMAP five-year data. The trispectrum has a negligible impact on the cosmological parameters for these simulations. For the cases where the weak lensing scaling parameter and the running of the spectral index are included the constraints on the cosmological parameters change by less than 10%.

B. The Weak Lensing Scaling Parameter

Using a prior ACBAR dataset, it was found that the weak lensing scaling parameter A_L is inconsistent with the expected value of unity at 2.5σ [15]. This led to an apparent revision by the ACBAR team and result-

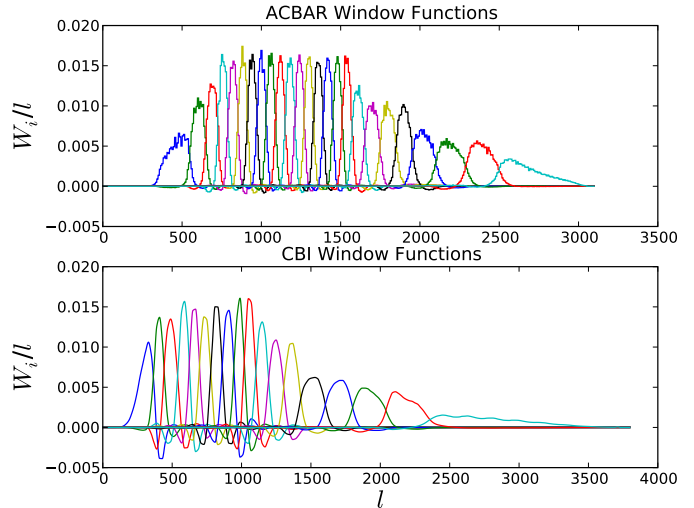


FIG. 4: The window functions used for our analysis of the ACBAR and CBI data sets.

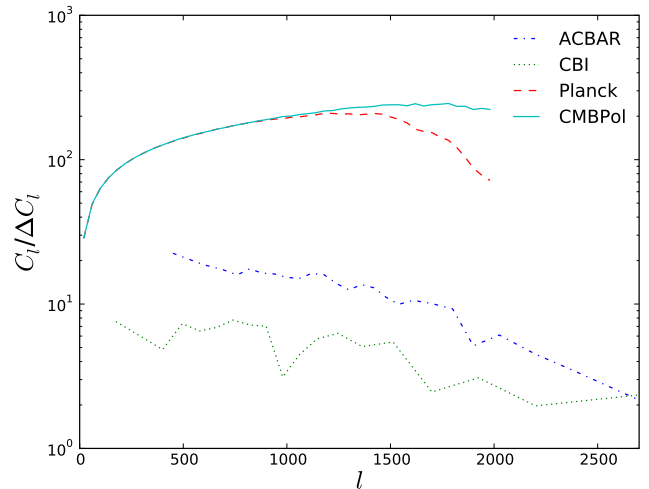


FIG. 5: The multipole-dependent ratio $C_l/\Delta C_l$ for the considered experiments (ACBAR in dot-dashed, CBI in dotted, Planck in dashed, and CMBPol in solid).

ing in a recalibration of the data. This apparently removed the result first demonstrated by Calabrese et al. [15] and the ACBAR team's own revised analysis showed A_L to be consistent with unity at a significance around 1.1σ [16]. However, given that this parameter is strongly sensitive to small angular scales where other secondary anisotropies contribute and non-Gaussianities become important, we have also chosen to include this parameter into our analysis. We have explicitly carried out two runs with this scaling parameter. For the first run, we incorporated A_L without any assumption of priors or the addition of other parameters, as shown in Table II. We find A_L to be consistent with unity at 1.4σ ,

TABLE II: The first column represents the cosmological parameters considered. In the second column we quantify the parameter constraints without non-Gaussian effects. The cosmological parameters determined from the combined ACBAR, CBI and WMAP five-year CMB data sets along with the non-Gaussian contributions from the trispectrum are shown in the third column. The same data without the trispectrum but with the variation of A_L is shown in the fifth column. The columns denoted $\Delta\sigma$ represent the percent change of the 1σ error bars.

Parameter	CMBData	CMBData+Tri.	$\Delta\sigma/\sigma$	CMBData+ A_L	$\Delta\sigma/\sigma$
$\Omega_b h^2$	0.02284 ± 0.00058	0.02283 ± 0.00059	2%	0.02300 ± 0.00063	9%
$\Omega_c h^2$	0.1103 ± 0.0060	0.1105 ± 0.0061	2%	0.1082 ± 0.0061	2%
θ	1.0408 ± 0.0026	1.0410 ± 0.0028	8%	1.0413 ± 0.0028	8%
τ	0.090 ± 0.017	0.089 ± 0.017	0%	0.090 ± 0.017	0%
n_s	0.966 ± 0.014	0.966 ± 0.015	7%	0.968 ± 0.015	7%
A_L	1	1	-	2.32 ± 0.93	-
$\log[10^{10} A_s]$	3.180 ± 0.047	3.178 ± 0.048	2%	3.166 ± 0.048	2%
Ω_Λ	0.741 ± 0.029	0.740 ± 0.029	0%	0.752 ± 0.030	3%
Age/GYr	13.67 ± 0.13	13.67 ± 0.14	8%	13.63 ± 0.14	8%
Ω_m	0.259 ± 0.029	0.259 ± 0.029	0%	0.247 ± 0.029	0%
σ_8	0.815 ± 0.031	0.801 ± 0.033	7%	0.789 ± 0.035	13%
z_{re}	10.5 ± 1.4	10.4 ± 1.4	0%	10.4 ± 1.4	0%
H_0	71.9 ± 2.6	71.8 ± 2.7	4%	73.1 ± 2.8	8%

TABLE III: In the second column, we quantify the cosmological parameter constraints incorporating the additional free parameters A_L and $dn_s/dlnk$. In the third column, we show the cosmological parameters determined from the combined ACBAR, CBI and WMAP 5-year CMB datasets with contributions from the trispectrum, along with the additional free parameters A_L and $dn_s/dlnk$.

Parameter	CMBData+ A_L +Run	CMBData+ A_L +Run+Tri.	$\Delta\sigma/\sigma$
$\Omega_b h^2$	0.02283 ± 0.00080	0.02269 ± 0.00081	2%
$\Omega_c h^2$	0.1135 ± 0.0089	0.1136 ± 0.0090	1%
θ	1.0410 ± 0.0029	1.0410 ± 0.0030	3%
τ	0.090 ± 0.017	0.090 ± 0.018	6%
n_s	0.997 ± 0.048	1.001 ± 0.049	2%
A_L	2.10 ± 0.90	2.02 ± 0.94	4%
$dn_s/dlnk$	-0.014 ± 0.024	-0.017 ± 0.025	4%
$\log[10^{10} A_s]$	3.167 ± 0.049	3.167 ± 0.049	0%
Ω_Λ	0.726 ± 0.047	0.723 ± 0.048	2%
Age/GYr	13.67 ± 0.16	13.69 ± 0.17	6%
Ω_m	0.275 ± 0.029	0.277 ± 0.029	0%
σ_8	0.810 ± 0.039	0.807 ± 0.041	5%
z_{re}	10.8 ± 1.5	10.8 ± 1.5	0%
H_0	71.0 ± 4.0	70.7 ± 4.1	3%

for the same reasons that the ACBAR team found this parameter to be consistent with the theoretical value in the fiducial cosmological model.

For the second simulation, in addition to A_L , we incorporated secondary non-Gaussianities and allowed the spectral index to run as this parameter is sensitive to physics on small scales. However, the constraint on the lensing amplitude remains unaffected. Nevertheless, it is possible that non-Gaussian effects are partly responsible for the inconsistency of the scaling parameter with unity, and future data sets with less noise on small angular scales are required to determine this.

C. Mock Runs

In order to understand the extent to which the trispectrum impacts the cosmological parameters in a prospective survey with less noise, we created TT mock datasets assuming the best fit WMAP5 cosmological parameters, with the optical depth fixed at $\tau = 0.087$, and with noise properties consistent with Planck's 143 GHz channel. Instead of considering cross-correlations, we only use the diagonal entries of the binned covariance matrix.

Table IV shows the results of the Planck mock simulation. Since Planck has significantly less noise at high

TABLE IV: In the second column, we show the cosmological parameter constraints from mock Planck data. In the third column, we quantify the non-Gaussianity induced shift of the best fit parameter values defined as the ratio of the parameter shift with the uncertainty. Simulation results combining the trispectrum with the Planck mock are shown in the third column.

Parameter	Planck	Planck + Tri.	$\Delta p_i/\sigma$	$\Delta\sigma$
$\Omega_b h^2$	0.02281 ± 0.00016	0.02271 ± 0.00018	-0.62	13%
$\Omega_c h^2$	0.1122 ± 0.0016	0.1132 ± 0.0018	0.63	12%
θ	1.04095 ± 0.00037	1.04084 ± 0.00044	-0.30	19%
n_s	0.9570 ± 0.0042	0.9538 ± 0.0047	-0.75	12%
$\log[10^{10} A_s]$	3.211 ± 0.017	3.224 ± 0.020	0.73	18%
Ω_Λ	0.7330 ± 0.0086	0.727 ± 0.010	-0.67	14%
Age/GYr	13.686 ± 0.028	13.704 ± 0.033	0.65	18%
Ω_m	0.2670 ± 0.0086	0.273 ± 0.010	0.67	14%
σ_8	0.8071 ± 0.0068	0.8113 ± 0.0076	-0.08	12%
z_{re}	10.395 ± 0.071	10.447 ± 0.081	0.74	14%
H_0	71.12 ± 0.76	70.62 ± 0.86	-0.67	13%

TABLE V: In the second column, we show the cosmological parameter constraints from mock CMBPol data. Simulation results combining the trispectrum with the CMBPol mock are shown in the third column.

Parameter	CMBPol	CMBPol + Tri.	$\Delta p_i/\sigma$	$\Delta\sigma$
$\Omega_b h^2$	0.02292 ± 0.00013	0.02279 ± 0.00016	-1.01	23%
$\Omega_c h^2$	0.1111 ± 0.0014	0.1126 ± 0.0017	1.09	21%
θ	1.04111 ± 0.00028	1.04110 ± 0.00036	-0.52	29%
n_s	0.9603 ± 0.0036	0.9558 ± 0.0044	-1.23	22%
$\log[10^{10} A_s]$	3.198 ± 0.015	3.216 ± 0.018	1.19	20%
Ω_Λ	0.7392 ± 0.0072	0.7309 ± 0.0091	-1.15	26%
Age/GYr	13.663 ± 0.023	13.689 ± 0.030	1.11	30%
Ω_m	0.2608 ± 0.0072	0.2691 ± 0.0091	1.09	26%
σ_8	0.8026 ± 0.0057	0.8088 ± 0.0071	-0.08	25%
z_{re}	10.336 ± 0.059	10.410 ± 0.073	1.25	24%
H_0	71.69 ± 0.65	70.95 ± 0.79	-1.15	22%

l , the trispectrum effects on the cosmological parameters is more apparent and the confidence regions of the most extreme changes are seen in Fig. 6. Here, the 1σ parameter constraints weaken by up to 20%. Thus, the trispectrum has a more significant impact for measuring the constraints on the cosmological parameters in experiments with a noise-level comparable to that of Planck on small angular scales.

Furthermore, in anticipation of CMBPol [30], which should have noise an order of magnitude less than Planck, we have carried out a mock CMBPol-like run with noise estimates consistent with the EPIC concept mission [31]. The results of this run are seen in Table V. For surveys with noise level comparable to that of CMBPol, non-Gaussian contributions in the trispectrum weaken the parameter constraints by up to 30%.

We have included in Table IV and Table V the parameter shifts induced in one realization of the mock CMB spectrum. Although the size of the parameter shifts extend up to 1.5σ , the shifts are not statistically significant as errors are correlated. We expect that for a set of real-

izations the shifts will cancel on average.

IV. CONCLUSIONS

Secondary non-Gaussianities in the trispectrum from weak lensing, the ISW effect, and the SZ effect have the potential to weaken the constraints on the cosmological parameters in experiments with high enough sensitivity to physics on small angular scales. While recent experiments such as ACBAR and CBI are too noisy for the trispectrum to become important at large multipoles, future surveys need to incorporate the trispectrum to avoid over-confident parameter estimation. The underlying cosmology constrained by Planck suffers a 20% degradation when these secondary contributions to the temperature anisotropies are properly incorporated, and this rises to 30% in CMBPol. Accounting for secondary non-Gaussianities in our analysis shows the weak lensing scaling parameter to be consistent with unity at 1.5σ .

Acknowledgments

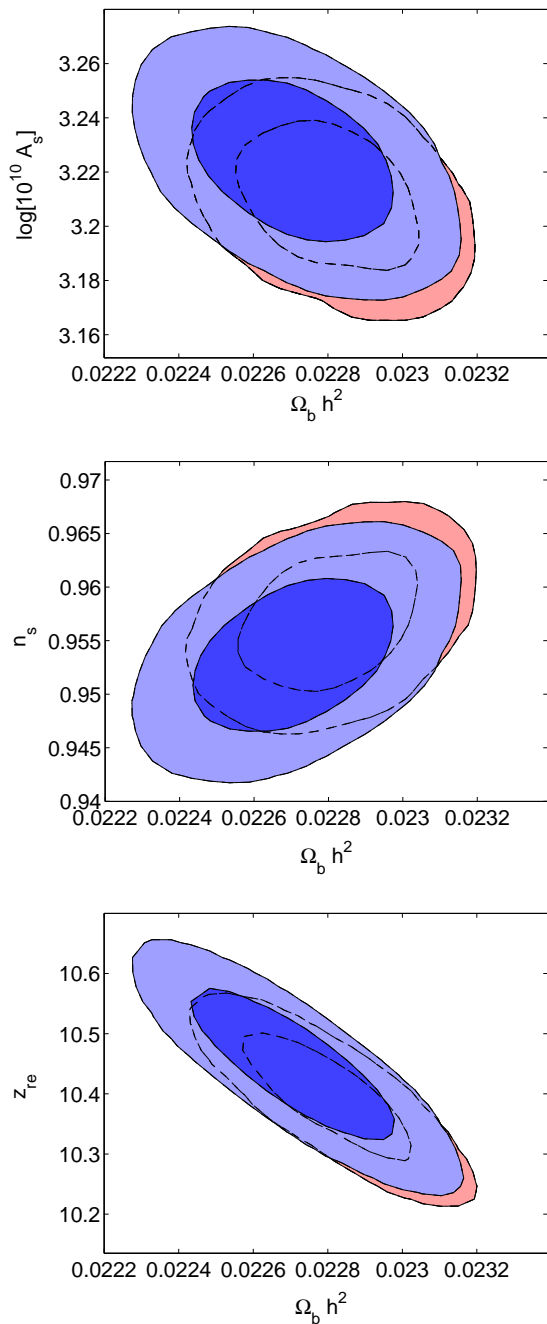


FIG. 6: The 68% and 95% confidence intervals in cosmological parameter constraints for the mock Planck run. These parameters are those with the largest shifts as seen in Table IV plotted against $\Omega_b h^2$. The red regions are those without the trispectrum, whereas the blue regions are those with the trispectrum.

We thank Erminia Calabrese, Eiichiro Komatsu, and Alessandro Melchiorri for helpful discussions. J.S. and S.J. acknowledge support from GAANN fellowships. This work was also supported by NSF AST-0645427.

[1] J. Dunkley *et al.* [WMAP Collaboration], *Astrophys. J. Suppl.* **180**, 306 (2009) [arXiv:0803.0586 [astro-ph]].
 [2] C. L. Reichardt *et al.*, *Astrophys. J.* **694**, 1200 (2009) [arXiv:0801.1491 [astro-ph]].

[3] J. L. Sievers *et al.*, arXiv:0901.4540 [astro-ph.CO].
 [4] W. Hu, *Phys. Rev. D* **62**, 043007 (2000) [arXiv:astro-ph/0001303].
 [5] M. Zaldarriaga, *Phys. Rev. D* **62**, 063510 (2000)

- [arXiv:astro-ph/9910498].
- [6] R. Scoccimarro, M. Zaldarriaga and L. Hui, *Astrophys. J.* **527**, 1 (1999) [arXiv:astro-ph/9901099].
- [7] A. Cooray and W. Hu, *Astrophys. J.* **554**, 56 (2001) [arXiv:astro-ph/0012087].
- [8] A. R. Cooray and W. Hu, *Astrophys. J.* **534**, 533 (2000) [arXiv:astro-ph/9910397].
- [9] D. N. Spergel and D. M. Goldberg, *Phys. Rev. D* **59**, 103001 (1999) [arXiv:astro-ph/9811252].
- [10] M. Zaldarriaga and U. Seljak, *Phys. Rev. D* **59**, 123507 (1999) [arXiv:astro-ph/9810257].
- [11] H. V. Peiris and D. N. Spergel, *Astrophys. J.* **540**, 605 (2000) [arXiv:astro-ph/0001393].
- [12] R. K. Sachs and A. M. Wolfe, *Astrophys. J.* **147**, 73 (1967).
- [13] R. A. Sunyaev and Y. B. Zeldovich, *Mon. Not. Roy. Astron. Soc.* **190**, 413 (1980).
- [14] A. Cooray, *Phys. Rev. D* **65**, 063512 (2002) [arXiv:astro-ph/0110415].
- [15] E. Calabrese, A. Slosar, A. Melchiorri, G. F. Smoot and O. Zahn, *Phys. Rev. D* **77**, 123531 (2008) [arXiv:0803.2309 [astro-ph]].
- [16] C. L. Reichardt *et al.*, *Astrophys. J.* **694**, 1200 (2009) [arXiv:0801.1491 [astro-ph]].
- [17] E. Komatsu and U. Seljak, *Mon. Not. Roy. Astron. Soc.* **336**, 1256 (2002) [arXiv:astro-ph/0205468].
- [18] A. Jenkins *et al.*, *Mon. Not. Roy. Astron. Soc.* **321**, 372 (2001) [arXiv:astro-ph/0005260].
- [19] D. J. Eisenstein and W. Hu, *Astrophys. J.* **511**, 5 (1997) [arXiv:astro-ph/9710252].
- [20] D. Limber, *Astrophys. J.* **119**, 655 (1954).
- [21] E. Komatsu and U. Seljak, *Mon. Not. Roy. Astron. Soc.* **327**, 1353 (2001) [arXiv:astro-ph/0106151].
- [22] A. Lewis and A. Challinor, *Phys. Rept.* **429**, 1 (2006) [arXiv:astro-ph/0601594].
- [23] M. Zaldarriaga and U. Seljak, *Phys. Rev. D* **58**, 023003 (1998) [arXiv:astro-ph/9803150].
- [24] E. Calabrese, A. Cooray, M. Martinelli, A. Melchiorri, L. Pagano, A. Slosar and G. F. Smoot, arXiv:0908.1585 [astro-ph.CO].
- [25] A. Cooray, *Phys. Rev. D* **64**, 063514 (2001) [arXiv:astro-ph/0105063].
- [26] A. Lewis and S. Bridle, *Phys. Rev. D* **66**, 103511 (2002) [arXiv:astro-ph/0205436].
- [27] A. Lewis, A. Challinor and A. Lasenby, *Astrophys. J.* **538**, 473 (2000) [arXiv:astro-ph/9911177].
- [28] E. Komatsu *et al.* [WMAP Collaboration], *Astrophys. J. Suppl.* **180**, 330 (2009) [arXiv:0803.0547 [astro-ph]].
- [29] A. Lewis and S. Bridle, *Phys. Rev. D* **66**, 103511 (2002) [arXiv:astro-ph/0205436].
- [30] D. Baumann *et al.* [CMBPol Study Team Collaboration], *AIP Conf. Proc.* **1141**, 10 (2009) [arXiv:0811.3919 [astro-ph]].
- [31] J. Bock *et al.* [EPIC Collaboration], arXiv:0906.1188 [astro-ph.CO]; J. Bock *et al.*, arXiv:0805.4207 [astro-ph].